

Thrust Distribution for 3-Jet Production from e^+e^- Annihilation within the QCD Conformal Window and in QED

Leonardo Di Giustino^{1,*}, Francesco Sannino^{2,3,4,†}, Sheng-Quan Wang^{5,‡} and Xing-Gang Wu^{6,§}

¹*Department of Science and High Technology, University of Insubria, via valleggio 11, I-22100, Como, Italy*

²*Scuola Superiore Meridionale, Largo S. Marcellino, 10, 80138 Napoli NA, Italy*

³*CP3-Origins & Danish IAS, Univ. of Southern Denmark, Campusvej 55, DK-5230 Odense*

⁴*Dipartimento di Fisica, E. Pancini, Università di Napoli Federico II, INFN sezione di Napoli, Complesso Universitario di Monte S. Angelo Edificio 6, via Cintia, 80126 Napoli, Italy*

⁵*Department of Physics, Guizhou Minzu University, Guiyang 550025, P.R. China and*

⁶*Department of Physics, Chongqing University, Chongqing 401331, P.R. China*

(Dated: April 27, 2021)

We investigate the theoretical predictions for thrust distribution in the electron positron annihilation to three-jets process at NNLO for different values of the number of flavors, N_f . To determine the distribution along the entire renormalization group flow from the highest energies to zero energy we consider the number of flavors near the upper boundary of the conformal window. In this regime of number of flavors the theory develops a perturbative infrared interacting fixed point. We then consider also the QED thrust obtained as the limit $N_c \rightarrow 0$ of the number of colors. In this case the low energy limit is governed by an infrared free theory. Using these quantum field theories limits as theoretical laboratories we arrive at an interesting comparison between the Conventional Scale Setting - (CSS) and the Principle of Maximum Conformality (PMC_∞) methods. We show that within the perturbative regime of the conformal window the two methods yield similar results while reducing the number of flavors towards the active number of flavors in the Standard Model the PMC_∞ method is the natural extension of the curves within the conformal window and best fits the data.

PACS numbers: 11.15.Bt, 11.10.Gh, 11.10.Jj, 12.38.Bx, 13.66.De, 13.66.Bc, 13.66.Jn

I. INTRODUCTION

We employ, for the first time, the perturbative regime of the QCD infrared conformal window as a laboratory to investigate in a controllable manner (near) conformal properties of physically relevant quantities such as the thrust distribution in electron positron annihilation processes.

The conformal window of QCD has a long and noble history conveniently summarised and generalised to arbitrary representations in Ref. [1]. This work led to renew interest in the subject and to a substantial number of lattice papers whose results and efforts that spanned a decade have been summarised in a recent report on the subject in Ref. [2].

When all quark masses are set to zero two physical parameters dictate the dynamic of the theory and these are the number of flavors and colors. Already at the one loop level one can distinguish two regimes of the theory. For the number of flavors larger than $11N_c/2$ the theory possesses an infrared non-interacting fixed point and at low energies the theory is known as non-abelian QED. The high energy fate of the theory is uncertain and it could de-

velop a critical number of flavors above which the theory reaches an UV fixed point [3] and therefore become safe. When the number of flavors is below $11N_c/2$ the non-interacting fixed point becomes UV in nature and then we say that the theory is asymptotically free. Lowering the number of flavors just below the point when asymptotic freedom is restored the theory develops a trustable infrared interacting fixed point discovered by Banks and Zaks [4] at two-loop level. The analysis at higher loops has been performed in [5–7]. As the number of flavors are further dropped it is widely expected that a quantum phase transition occurs with its nature, dynamics and potential universal behavior still unknown [2]. The fate at substantially lower number of matter fields is, however, clear given that we observe chiral symmetry breaking, and therefore a dynamical scale is dynamically generated yielding the bulk of all the known hadron masses. The two-dimensional region in the number of flavors and colors where asymptotically free QCD develops an IR interacting fixed point is colloquially known as the conformal window of QCD. In this work we will consider the region of flavors and colors near the upper bound of the conformal window where the IR fixed point can be reliably accessed in perturbation theory.

Next we move to discuss the thrust distribution and the Event Shape variables that are a fundamental tool in order to probe the geometrical structure of a given process at colliders. In fact, while cross sections are too inclusive with respect to the final state leading to simple geometrical information on the process, jet rates and

*email:leonardo.digiustino@gmail.com

†email:sannino@cp3.sdu.dk

‡email:sqwang@cqu.edu.cn

§email:wuxg@cqu.edu.cn

Event Shape variables are exclusive enough quantities that allow for a deeper geometrical analysis of the process. Since the e^+e^- to three-jets process starts already at $O(\alpha_s)$, Event Shapes variables are also particularly suitable for the measurement of the strong coupling α_s . In fact, they have been extensively used for this purpose [8].

Given the large amount of data collected at LEP and SLAC [9–13], refined calculations are crucial in order to extract information to the highest possible precision. One of the obstacles in making precise predictions for the hadron production quantities is the large renormalization energy scale ambiguity which leads to significant theoretical uncertainties. Though extensive studies on the Event Shape variables have been released during the last decades including higher order corrections from next-to-leading order (NLO) calculations [14–19] to the next-to-next-to-leading order (NNLO) [20–24] and including resummation of the large logarithms [25, 26], the scale uncertainties are still dominant. In the particular case of the three-jet event shape distributions the conventional practice (Conventional Scale Setting - CSS) of fixing the renormalization scale to the center-of-mass energy $\mu_r = \sqrt{s}$, and of evaluating the uncertainties by varying the scale within an arbitrary range, e.g. $\mu_r \in [\sqrt{s}/2, 2\sqrt{s}]$ lead to results that do not match the experimental data and the extracted values of α_s deviate from the world average [27]. Additionally, the conventional scale setting procedure is not consistent with the Gell-Mann-Low scheme [28] in Quantum Electrodynamics (QED) and it is affected by scheme dependence for the pQCD predictions violating a fundamental principle of the renormalization group invariance.

The resulting perturbative series is also factorially divergent at large orders like $n!\beta_0^n\alpha_s^n$ the "renormalon" problem [29], with β_0 the first beta function coefficient. Given the factorial growth, the hope to suppress scale uncertainties by including higher-order corrections is compromised. A solution to the scale ambiguity problem is offered by the *Principle of Maximum Conformality* (PMC) [30–35]. This method provides a systematic way to eliminate renormalization scheme-and-scale ambiguities. Since the PMC predictions do not depend on the choice of the renormalization scheme, PMC scale setting satisfies the principles of renormalization group invariance [36, 37]. The PMC procedure is consistent with the standard Gell-Mann-Low method in the Abelian limit, $N_c \rightarrow 0$ [38]. The method further determines the renormalization scale by absorbing the β terms that govern the behavior of the running coupling via the renormalization group equation. The divergent renormalon terms cancel and the convergence of pQCD is greatly improved. Besides in a theory of unification of all forces, electromagnetic, weak and strong interactions, such as the Standard Model, or either of Grand Unification, one cannot simply apply a different scale-setting or analytic procedure to different sectors of the theory. The PMC offers the possibility to apply

the same method in all sectors of the Standard Model starting from first principles, eliminating the renormalon growth, the scheme dependence, the scale ambiguity, and satisfying the QED constraint in the zero-color limit $N_c \rightarrow 0$.

In particular recent applications of the PMC and of the PMC_∞ have shown to significantly reduce the theoretical errors in Event Shape Variable distributions highly improving also the fit with the experimental data [41] and to improve the theoretical prediction on the $\alpha_s(M_{Z_0})$ respect to the world average [39][40].

It is highly desirable to test these methods along the entire renormalization group flow from the highest energies down to zero energy. This is precluded in standard QCD with a number of active flavors less than six because the theory becomes strongly coupled at low energies. We therefore employ the perturbative regime of the conformal window which allows us to arrive at arbitrary low energies and obtain the corresponding results for the $\text{SU}(N_c)$ thrust with $N_c = 3$ at the cost of increasing the number of active flavors near the loss of asymptotic freedom value of $11N_c/2$. Here we are able to deduce the full solution at NNLO in the strong coupling. We consider also the $\text{U}(1)$ abelian QED thrust distribution which rather than being infrared interacting is infrared free. We conclude by presenting the comparison between two renormalization scale methods, the CSS and the PMC_∞ .

A. The Strong Coupling at NNLO

The value of the QCD strong coupling α_s at different energies μ can be computed via its β -function

$$\mu^2 \frac{d}{d\mu^2} \left(\frac{\alpha_s}{2\pi} \right) = -\frac{1}{2}\beta_0 \left(\frac{\alpha_s}{2\pi} \right)^2 - \frac{1}{4}\beta_1 \left(\frac{\alpha_s}{2\pi} \right)^3 + O(\alpha_s^4) \quad (1)$$

with :

$$\beta_0 = \frac{11}{3}C_A - \frac{4}{3}T_R N_f \quad (2)$$

$$\beta_1 = \frac{34}{3}C_A^2 - 4 \left(\frac{5}{3}C_A + C_F \right) T_R N_f \quad (3)$$

where $C_F = \frac{(N_c^2 - 1)}{2N_c}$, $C_A = N_c$ and $T_R = 1/2$. Being this a first order differential equation we need an initial value of α_s at a given energy scale. This value is determined phenomenologically. In QCD the number of colors N_c is set to 3, while the N_f , i.e. the number of active flavors, varies across the quark mass thresholds. In this work we determine the evolution of the strong coupling keeping the number of colors to $N_c \equiv 3$ while varying the number of flavors within the perturbative regime of the conformal window. We will then consider the QED thrust distribution by performing the Abelian limit $N_c \rightarrow 0$. We will then apply the PMC_∞ method for the renormalization of the fine structure constant α and compare the

QED and QCD results among themselves and with the phenomenological data.

B. Two-loop results

In order to determine the solution for the strong coupling α_s evolution we first introduce the following notation: $x(\mu) \equiv \frac{\alpha_s(\mu)}{2\pi}$, $t = \log(\mu^2/\mu_0^2)$, $B = \frac{1}{2}\beta_0$ and $C = \frac{1}{2}\frac{\beta_1}{\beta_0}$. The truncated NNLO approximation of the Eq.1 leads to the differential equation:

$$\frac{dx}{dt} = -Bx^2(1 + Cx) \quad (4)$$

An implicit solution of Eq.4 is given by the Lambert $W(z)$ function:

$$We^W = z \quad (5)$$

with:

$$W = \left(-\frac{1}{Cx} - 1 \right) \quad (6)$$

$$z = e^{-\frac{1}{Cx_0}-1} \left(-\frac{1}{Cx_0} - 1 \right) \left(\frac{\mu^2}{\mu_0^2} \right)^{-\frac{B}{C}}. \quad (7)$$

The general solution for the coupling is:

$$x = -\frac{1}{C} \frac{1}{1 + W}. \quad (8)$$

In order to discuss the different branches we adopt the notation: $x^* \equiv -\frac{1}{C}$, which follows

$$x = \frac{x^*}{1 + W}, \quad (9)$$

$$z = e^{\frac{x^*}{x_0}-1} \left(\frac{x^*}{x_0} - 1 \right) \left(\frac{\mu^2}{\mu_0^2} \right)^{x^*B}, \quad (10)$$

and we will refer to the initial value $x_0 \equiv \alpha_s(M_{Z_0})/(2\pi) \simeq 0.01880 \pm 0.00021$ given by the coupling determined at the Z_0 mass scale.

In the range $N_f < \frac{34N_c^3}{13N_c^2-3}$ and $N_f > \frac{11}{2}N_c$ we have that the solution is given by the W_{-1} branch, while for $\frac{34N_c^3}{13N_c^2-3} < N_f < \frac{11}{2}N_c$ the solution for the strong coupling is given by the W_0 branch. By introducing the phenomenological value x_0 , we define a restricted range for the IR fixed point respect to the Banks-Zaks [4] discussion. Given the value $\bar{N}_f = x^{*-1}(x_0) \simeq 15.219 \pm 0.012$, we have that in the range $\frac{34N_c^3}{13N_c^2-3} < N_f < \bar{N}_f$ the β -function has both a UV and an IR fixed point, while for $N_f > \bar{N}_f$ we no longer have the correct UV behavior compatible with the phenomenological initial value of the coupling. In other words for N_f in between \bar{N}_f and $\frac{11}{2}N_c$ the IR fixed point value is always smaller than the one at the Z_0 scale.

Thus the actual physical range of a conformal window for QCD is given by $\frac{34N_c^3}{13N_c^2-3} < N_f < \bar{N}_f$.

The behavior of the coupling is shown in Fig.1. In the IR region the strong coupling approaches the IR finite limit in the case of values of N_f within the conformal window (e.g. Black Dashed curve of Fig. 1), while it diverges at

$$\Lambda = \mu_0 \left(1 + \frac{|x^*|}{x_0} \right)^{\frac{1}{2B|x^*|}} e^{-\frac{1}{2Bx_0}} \quad (11)$$

outside the conformal window given the solution for the coupling with W_{-1} (e.g. Solid Red curve of Fig.1). We underline that the presence of a Landau "ghost" pole in the strong coupling is only an effect of the breaking of the perturbative regime, including non-perturbative contributions, or using non-perturbative QCD, a finite limit is expected at any N_f [46]. Both solutions have the correct UV asymptotic free behavior. For the case $\bar{N}_f < N_f < \frac{11}{2}N_c$, though we have a negative z and a multi-valued solution, one real and the other imaginary, actually only one (the real) is acceptable given the initial conditions, but this solution is not asymptotically free. Thus we restrict our analysis to the range $N_f < \bar{N}_f$ where we have the correct UV behavior. In general IR and UV fixed points of the β -function can also be determined at different values of the number of colors N_c (different gauge group $SU(N)$) and N_f extending this analysis also to other gauge theories; in particular this has been investigated for the $\mathcal{N} = 1$ super symmetric gauge theory in Ref. [45].

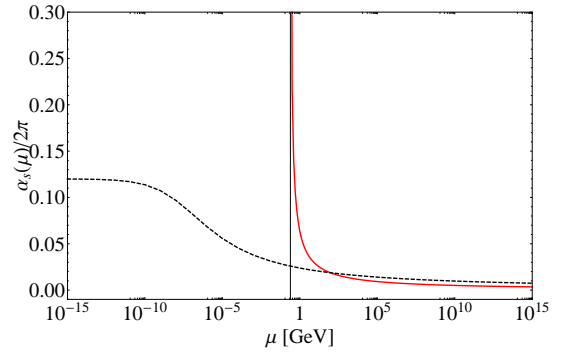


FIG. 1: The strong running coupling $\alpha_s(\mu)$ for $N_f = 12$ (Black Dashed) and for $N_f = 5$ (Solid Red).

C. Thrust at NNLO

The thrust (T) variable is defined as

$$T = \frac{\max_{\vec{n}} \sum_i |\vec{p}_i \cdot \vec{n}|}{\sum_i |\vec{p}_i|}, \quad (12)$$

where the sum runs over all particles in the hadronic final state, and the \vec{p}_i denotes the three-momentum of particle

i . The unit vector \vec{n} is varied to maximize thrust T , and the corresponding \vec{n} is called the thrust axis and denoted by \vec{n}_T . It is often used the variable $(1 - T)$, which for the LO of the 3jet production is restricted to the range $(0 < 1 - T < 1/3)$. Respectively we have a back-to-back or a spherically symmetric event respectively at $T = 1$ and at $T = 2/3$.

In general a normalized IR safe single variable observable, such as the thrust distribution for the $e^+e^- \rightarrow 3jets$ [42, 43], is the sum of pQCD contributions calculated up to NNLO at the initial renormalization scale $\mu_0 = \sqrt{s} = M_{Z_0}$:

$$\frac{1}{\sigma_{tot}} \frac{Od\sigma(\mu_0)}{dO} = \left\{ \frac{\alpha_s(\mu_0)}{2\pi} \frac{Od\bar{A}_O(\mu_0)}{dO} + \left(\frac{\alpha_s(\mu_0)}{2\pi} \right)^2 \frac{Od\bar{B}_O(\mu_0)}{dO} + \left(\frac{\alpha_s(\mu_0)}{2\pi} \right)^3 \frac{Od\bar{C}_O(\mu_0)}{dO} + \mathcal{O}(\alpha_s^4) \right\}, \quad (13)$$

where O is the selected Event Shape variable,

$$\sigma_{tot} = \sigma_0 \left(1 + \frac{\alpha_s(\mu_0)}{2\pi} A_{tot} + \left(\frac{\alpha_s(\mu_0)}{2\pi} \right)^2 B_{tot} + \mathcal{O}(\alpha_s^3) \right)$$

is total hadronic cross section and $\bar{A}_O, \bar{B}_O, \bar{C}_O$ are respectively the normalized LO, NLO and NNLO coefficients.

$$\bar{A}_O = A_O \quad (14)$$

$$\bar{B}_O = B_O - A_{tot} A_O \quad (15)$$

$$\bar{C}_O = C_O - A_{tot} B_O - (B_{tot} - A_{tot}^2) A_O \quad (16)$$

where A_O, B_O, C_O are the coefficients normalized to the tree level cross section σ_0 calculated by Monte-Carlo (see e.g. EERAD and Event2 codes [20–24]) and A_{tot}, B_{tot} are:

$$A_{tot} = \frac{3}{2} C_F; \quad (17)$$

$$B_{tot} = \frac{C_F}{4} N_c + \frac{3}{4} C_F \frac{\beta_0}{2} (11 - 8\zeta(3)) - \frac{3}{8} C_F^2. \quad (18)$$

In general according to conventional practice the renormalization scale is set $\mu_R \equiv \sqrt{s}$ and then errors are calculated varying the scale in the range $\sqrt{s}/2 < \mu_R < 2\sqrt{s}$.

According to the PMC_∞ (for an introduction on the PMC_∞ see Ref.[41]) Eq.13 becomes:

$$\frac{1}{\sigma_{tot}} \frac{Od\sigma(\mu_I, \mu_{II}, \mu_0)}{dO} = \{ \bar{\sigma}_I + \bar{\sigma}_{II} + \bar{\sigma}_{III} + \mathcal{O}(\alpha_s^4) \}, \quad (19)$$

where the $\bar{\sigma}_N$ are normalized subsets that in the region $(1 - T) < 0.33$ are given by:

$$\bar{\sigma}_I = A_{Conf} \frac{\alpha_I}{2\pi}$$

$$\bar{\sigma}_{II} = (B_{Conf} + \eta A_{tot} A_{Conf}) \left(\frac{\alpha_{II}}{2\pi} \right)^2 - \eta A_{tot} A_{Conf} \left(\frac{\alpha_0}{2\pi} \right)^2$$

$$-A_{tot} A_{Conf} \frac{\alpha_0}{2\pi} \frac{\alpha_I}{2\pi}$$

$$\bar{\sigma}_{III} = (C_{Conf} - A_{tot} B_{Conf} - (B_{tot} - A_{tot}^2) A_{Conf}) \left(\frac{\alpha_0}{2\pi} \right)^3, \quad (20)$$

$A_{Conf}, B_{Conf}, C_{Conf}$ are the scale invariant conformal coefficients (i.e. the coefficients of each perturbative order not depending on the scale μ_R) while $\alpha_I, \alpha_{II}, \alpha_0$ are the couplings determined at the μ_I, μ_{II}, M_{Z_0} scales respectively. The η parameter is a regularization term in order to cancel the singularities of the NLO scale depending on non-matching zeroes between numerator and denominator in the C_{β_0} . In general this term is not mandatory for applying the PMC_∞ , it is necessary only in case one is interested to apply the method all over an entire spectrum of a given variable. Its value has been determined to $\eta = 3.51$ for the thrust distribution and it introduces no bias effects up to the accuracy of the calculation and the related errors are totally negligible up to this stage.

The PMC_∞ scales, μ_N , are given by :

$$\mu_I = \sqrt{s} \cdot e^{-\frac{1}{2} B_{\beta_0}}, \quad (1-T) < 0.33 \quad (21)$$

$$\tilde{\mu}_{II} = \begin{cases} \sqrt{s} \cdot e^{-\frac{1}{2} C_{\beta_0} \cdot \frac{B_{Conf}}{B_{Conf} + \eta \cdot A_{tot} A_{Conf}}}, & (1-T) < 0.33 \\ \sqrt{s} \cdot e^{-\frac{1}{2} \left(\frac{C_1}{11B_1 - \frac{2}{3}B_0} \right)}, & (1-T) > 0.33 \end{cases} \quad (22)$$

they don't change varying the number of flavors N_f , and they are shown in Fig.2. The coefficients B_{β_0}, C_{β_0} are the coefficients related to the β_0 -terms of each perturbative order, and are determined from the calculated A_O, B_O, C_O coefficients by using the iCF (*the Intrinsic Conformality* [41]). The coefficients B_1, C_1 are the NLO and NNLO coefficients of the N_f terms, while the B_0 is the remaining term of the NLO coefficient.

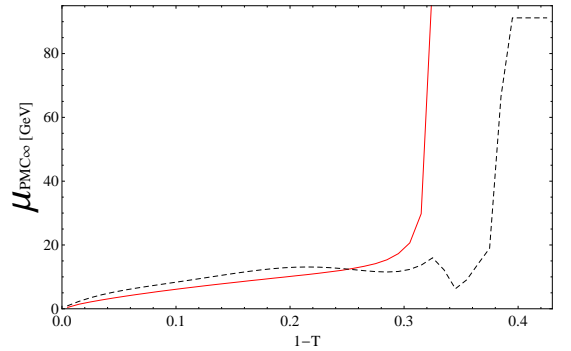


FIG. 2: The LO- PMC_∞ (Solid Red) and the NLO- PMC_∞ (Dashed Black) scales for thrust.

II. THE THRUST DISTRIBUTION ACCORDING TO N_f

Results for the thrust distribution calculated using the NNLO solution for the coupling $\alpha_s(\mu)$, at different values of the number of flavors, N_f , is shown in Fig.3. A direct comparison between PMC_∞ (Solid line) and Conventional Scale Setting (Dashed line) is shown at different values of the number of flavors. We notice that the PMC_∞ is the natural extension of the conformal distribution outside the conformal window. In fact, the position of the peak is rather preserved varying the N_f in and out of the conformal window using the PMC_∞ , while there is shift towards lower values using the CSS. Furthermore the direct comparison with the experimental data shows that the PMC_∞ determines the correct number of flavor $5 < N_f(1-T) < 6$ (Gray shaded area Fig.3) dynamically all over the spectrum of the $(1-T)$ variable. While in the central range of the conformal window $12 < N_f < 15$ (Yellow shaded area Fig.3), there is good overlap of the predictions according to CSS and to PMC_∞ , as expected from general grounds.

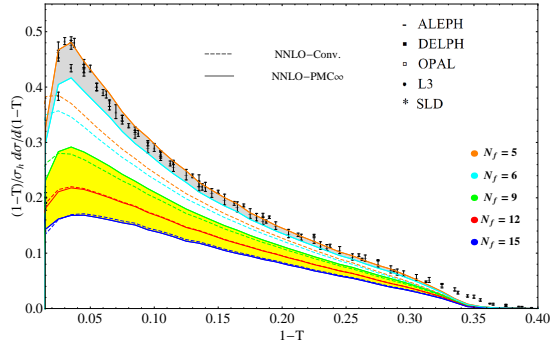


FIG. 3: Thrust distributions for different values of N_f , using the PMC_∞ (Solid line) and the Conventional Scale Setting (Dashed line). The Yellow shaded area are the results for the values of N_f taken in the conformal window. The experimental data points are taken from the ALEPH, DELPHI, OPAL, L3, SLD experiments [9–13].

III. THE THRUST DISTRIBUTION IN THE ABELIAN LIMIT $N_c \rightarrow 0$

We obtain the QED thrust distribution performing the $N_c \rightarrow 0$ limit of the QCD thrust at NNLO accordingly to [38, 44]. In the zero number of colors limit the gauge group color factors are fixed by $N_A = 1, C_F = 1, T_R = 1, C_A = 0, N_A = 0, N_f = N_l$ while the β -terms and the coupling rescale as β_n/C_F^{n+1} and $\alpha_s \cdot C_F$ respectively. In particular $\beta_0 = -\frac{4}{3}N_l$ and $\beta_1 = -4N_l$ using the normalization of Eq.1. According to these rescaling of the color factors we have determined the QED thrust and the QED PMC_∞ scales. For the QED coupling, we have used the analytic formula for the effective fine structure constant

in the $\overline{\text{MS}}$ -scheme:

$$\alpha(Q^2) = \frac{\alpha}{(1 - \Re \Pi^{\overline{\text{MS}}}(Q^2))}, \quad (23)$$

with $\alpha^{-1} \equiv \alpha(0)^{-1} = 137.036$ and the vacuum polarization function (VPF) calculated perturbatively at two loops including contributions from leptons, quarks and W boson.

The QED PMC_∞ scales are :

$$\mu_I = \sqrt{s} \cdot e^{\frac{5}{6} - \frac{1}{2} B \beta_0}, \quad (1-T) < 0.33 \quad (24)$$

$$\tilde{\mu}_{II} = \begin{cases} \sqrt{s} \cdot e^{\frac{5}{6} - \frac{1}{2} C \beta_0 \cdot \frac{B_{\text{Conf}}}{B_{\text{Conf}} + \eta \cdot A_{\text{tot}} A_{\text{Conf}}}}, & (1-T) < 0.33 \\ \sqrt{s} \cdot e^{\frac{5}{6} - \frac{1}{2} \left(\frac{C_1}{-\frac{4}{3} B_0} \right)}, & (1-T) > 0.33 \end{cases}, \quad (25)$$

the η regularization parameter introduced to cancel singularities in the NLO PMC_∞ scale, μ_{II} in the $N_c \rightarrow 0$ limit tends to the same QCD value, $\eta = 3.51$. Plot of the PMC_∞ scales is shown in Fig.4. We notice that in the QED limit the PMC_∞ scales have analogous dynamical behavior as those calculated in QCD, differences arise by the $\overline{\text{MS}}$ scheme factor reabsorption and at NLO by the N_c number of colors effect. Thus we notice that perfect consistency is shown from QCD to QED using the PMC_∞ method.

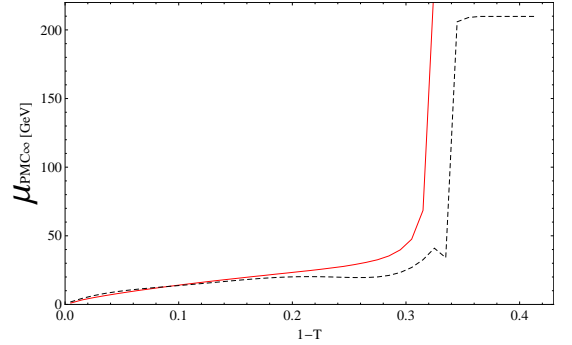


FIG. 4: LO- PMC_∞ (Solid Red) the NLO- PMC_∞ (Dashed Black) scales for the Abelian limit of the thrust distribution.

The normalized QED thrust distribution is shown in Fig. 5. We notice that the curve is peaked at the origin, $T = 1$, which suggests that the three jet event in QED occurs with a rather back-to-back symmetry. Results for the CSS and the PMC_∞ methods in QED are of the order of $O(\alpha)$ and given the good convergence of the theory the results for the two methods show very small differences.

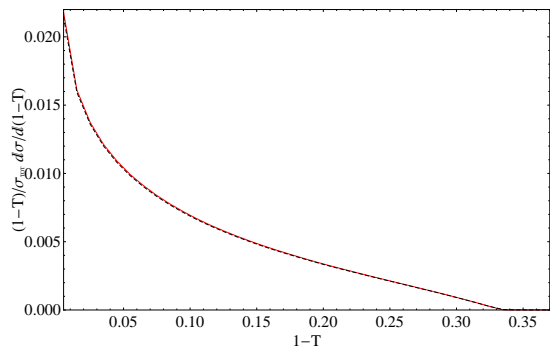


FIG. 5: Thrust distributions in the QED limit at NNLO using the PMC_∞ (Solid Red) and the Conventional Scale Setting (Dashed Black).

IV. CONCLUSIONS

We have investigated, for the first time, the thrust distribution in the QCD conformal window. Assuming, for phenomenological reasons, the physical value of the

strong coupling to be the one at the Z_0 mass scale it restricts the conformal window range, at two loops, to be within $\frac{34N_c^3}{13N_c^2-3} < N_f < \bar{N}_f$ with $\bar{N} \simeq 15.22$. The closer N_f to the higher value the more perturbative the system is.

Results for the thrust distribution in the conformal window show that the PMC_∞ method can be considered as the natural extension of the conformal distribution out of the conformal window. Comparison with the experimental data indicates also that PMC_∞ agrees with the expected number of flavors. A good fit with experimental data is shown by the PMC_∞ results for the range $5 < N_f < 6$, which agrees with the active number of flavors of the Standard Model. In addition, calculations for the QED thrust reveal a perfect consistency of the PMC_∞ with QED when taking the Abelian limit of QCD for both the PMC_∞ scale and for the regularization η parameter which tends to the same QCD value.

Acknowledgements: We thank Stanley J. Brodsky for his valuable comments and for useful discussions.

-
- [1] D. D. Dietrich and F. Sannino, Phys. Rev. D **75** (2007), 085018 doi:10.1103/PhysRevD.75.085018 [arXiv:hep-ph/0611341 [hep-ph]].
 - [2] G. Cacciapaglia, C. Pica and F. Sannino, Phys. Rept. **877** (2020), 1-70 doi:10.1016/j.physrep.2020.07.002 [arXiv:2002.04914 [hep-ph]].
 - [3] O. Antipin and F. Sannino, Phys. Rev. D **97** (2018) no.11, 116007 doi:10.1103/PhysRevD.97.116007 [arXiv:1709.02354 [hep-ph]].
 - [4] T. Banks, A. Zaks, Nuclear Physics B. Elsevier BV. **196** (2): 189-204 (1982).
 - [5] C. Pica and F. Sannino, Phys. Rev. D **83** (2011), 035013 doi:10.1103/PhysRevD.83.035013 [arXiv:1011.5917 [hep-ph]].
 - [6] T. A. Ryttov and R. Shrock, Phys. Rev. D **83** (2011), 056011 doi:10.1103/PhysRevD.83.056011 [arXiv:1011.4542 [hep-ph]].
 - [7] T. A. Ryttov and R. Shrock, Phys. Rev. D **94** (2016) no.10, 105015 doi:10.1103/PhysRevD.94.105015 [arXiv:1607.06866 [hep-th]].
 - [8] S. Kluth, Rept. Prog. Phys. **69**, 1771 (2006).
 - [9] A. Heister *et al.* [ALEPH Collaboration], Eur. Phys. J. C **35**, 457 (2004).
 - [10] J. Abdallah *et al.* [DELPHI Collaboration], Eur. Phys. J. C **29**, 285 (2003).
 - [11] G. Abbiendi *et al.* [OPAL Collaboration], Eur. Phys. J. C **40**, 287 (2005).
 - [12] P. Achard *et al.* [L3 Collaboration], Phys. Rept. **399**, 71 (2004).
 - [13] K. Abe *et al.* [SLD Collaboration], Phys. Rev. D **51**, 962 (1995).
 - [14] R. K. Ellis, D. A. Ross and A. E. Terrano, Nucl. Phys. B **178**, 421 (1981).
 - [15] Z. Kunszt, Phys. Lett. **99B**, 429 (1981).
 - [16] J. A. M. Vermaseren, K. J. F. Gaemers and S. J. Oldham, Nucl. Phys. B **187**, 301 (1981).
 - [17] K. Fabricius, I. Schmitt, G. Kramer and G. Schierholz, Z. Phys. C **11**, 315 (1981).
 - [18] W. T. Giele and E. W. N. Glover, Phys. Rev. D **46**, 1980 (1992).
 - [19] S. Catani and M. H. Seymour, Phys. Lett. B **378**, 287 (1996).
 - [20] A. Gehrmann-De Ridder, T. Gehrmann, E. W. N. Glover and G. Heinrich, Phys. Rev. Lett. **99**, 132002 (2007).
 - [21] A. Gehrmann-De Ridder, T. Gehrmann, E. W. N. Glover and G. Heinrich, JHEP **0712**, 094 (2007).
 - [22] A. Gehrmann-De Ridder, T. Gehrmann, E. W. N. Glover and G. Heinrich, Comput. Phys. Commun. **185**, 3331 (2014).
 - [23] S. Weinzierl, Phys. Rev. Lett. **101**, 162001 (2008).
 - [24] S. Weinzierl, JHEP **0906**, 041 (2009).
 - [25] R. Abbate, M. Fickinger, A. H. Hoang, V. Mateu and I. W. Stewart, Phys. Rev. D **83**, 074021 (2011).
 - [26] A. Banfi, H. McAslan, P. F. Monni and G. Zanderighi, JHEP **1505**, 102 (2015).
 - [27] M. Tanabashi *et al.* [Particle Data Group], Phys. Rev. D **98**, 030001 (2018).
 - [28] M. Gell-Mann and F. E. Low, Phys. Rev. **95**, 1300 (1954).
 - [29] M. Beneke, Phys. Rept. **317**, 1 (1999).
 - [30] S. J. Brodsky, G. P. Lepage and P. B. Mackenzie, Phys. Rev. D **28**, 228 (1983) doi:10.1103/PhysRevD.28.228
 - [31] S. J. Brodsky and L. Di Giustino, Phys. Rev. D **86**, 085026 (2012).
 - [32] S. J. Brodsky and X. G. Wu, Phys. Rev. D **85**, 034038 (2012).
 - [33] S. J. Brodsky and X. G. Wu, Phys. Rev. Lett. **109**, 042002 (2012).
 - [34] M. Mojaza, S. J. Brodsky and X. G. Wu, Phys. Rev. Lett. **110**, 192001 (2013).
 - [35] S. J. Brodsky, M. Mojaza and X. G. Wu, Phys. Rev. D

- 89**, 014027 (2014).
- [36] S. J. Brodsky and X. G. Wu, Phys. Rev. D **86**, 054018 (2012).
 - [37] X. G. Wu, Y. Ma, S. Q. Wang, H. B. Fu, H. H. Ma, S. J. Brodsky and M. Mojaza, Rept. Prog. Phys. **78**, 126201 (2015).
 - [38] S. J. Brodsky and P. Huet, Phys. Lett. B **417**, 145 (1998).
 - [39] S. Q. Wang, S. J. Brodsky, X. G. Wu and L. Di Giustino, Phys. Rev. D **99**, no.11, 114020 (2019) doi:10.1103/PhysRevD.99.114020 [arXiv:1902.01984 [hep-ph]].
 - [40] S. Q. Wang, S. J. Brodsky, X. G. Wu, J. M. Shen and L. Di Giustino, Phys. Rev. D **100**, no.9, 094010 (2019) doi:10.1103/PhysRevD.100.094010 [arXiv:1908.00060 [hep-ph]].
 - [41] L. Di Giustino, S. J. Brodsky, S. Q. Wang and X. G. Wu, Phys. Rev. D **102**, no.1, 014015 (2020) doi:10.1103/PhysRevD.102.014015 [arXiv:2002.01789 [hep-ph]].
 - [42] V. Del Duca, C. Duhr, A. Kardos, G. Somogyi and Z. Trocsanyi, Phys. Rev. Lett. **117**, 152004 (2016).
 - [43] V. Del Duca, C. Duhr, A. Kardos, G. Somogyi, Z. Szor, Z. Trocsanyi and Z. Tulipant, Phys. Rev. D **94**, 074019 (2016).
 - [44] A. L. Kataev and V. S. Molokoedov, Phys. Rev. D **92**, no.5, 054008 (2015) doi:10.1103/PhysRevD.92.054008 [arXiv:1507.03547 [hep-ph]].
 - [45] T. A. Rytov and R. Shrock, Phys. Rev. D **96**, no.10, 105018 (2017) doi:10.1103/PhysRevD.96.105018 [arXiv:1706.06422 [hep-th]].
 - [46] A. Deur, S. J. Brodsky and G. F. de Teramond, Nucl. Phys. **90**, 1 (2016) doi:10.1016/j.ppnp.2016.04.003 [arXiv:1604.08082 [hep-ph]].